Steel and Composite Structures, Vol. 1, No. 3 (2001) 329-340
DOI: http://dx.doi.org/10.12989/scs.2001.1.3.329

Seismic design of connections between steel outrigger beams and reinforced concrete walls

Jeremy T. Deason†

LJB Engineers, 3100 Research Blvd., P.O. Box 20246, Dayton, OH 45420-0246, U.S.A.

Gokhan Tunc†

Cantor Seinuk Group, Inc. (WSP), 600 Madison Avenue, New York, NY 10022, U.S.A.

Bahram M. Shahrooz‡

Department of Civil and Environmental Engineering, University of Cincinnati, P.O. Box 210071, Cincinnati, OH 45221-0071, U.S.A.

Abstract. Cyclic response of "shear" connections between steel outrigger beams and reinforced concrete core walls is presented in this paper. The connections investigated in this paper consisted of a shear tab welded onto a plate that was connected to the core walls through multiple headed studs. The experimental data from six specimens point to a capacity larger than the design value. However, the mode of failure was through pullout of the embedded plate, or fracture of the weld between the studs and plate. Such brittle modes of failure need to be avoided through proper design. A capacity design method based on dissipating the input energy through yielding and fracture of the shear tab was developed. This approach requires a good understanding of the expected capacity of headed studs under combined gravity shear and cyclic axial load (tension and compression). A model was developed and verified against test results from six specimens. A specimen designed based on the proposed design methodology performed very well, and the connection did not fail until shear tab fractured after extensive yielding. The proposed design method is recommended for design of outrigger beam-wall connections.

Key words: collector element; composite construction; cyclic testing; floor diaphragm; hybrid structures; outrigger beam; reinforced concrete wall; shear stud; walls.

1. Introduction

A common hybrid structural system involves the use of reinforced concrete core walls, which are formed by coupling a number of individual walls, and steel perimeter frame. Fig. 1 illustrates a typical floor plan of such a hybrid structural system. The structural core walls are used to provide the necessary lateral load strength and stiffness. For low-to-moderate rise buildings up to 25 to 30 stories, the core walls are the primary lateral load resisting system, and the perimeter frame is designed for gravity

†Structural Engineer
‡Associate Professor

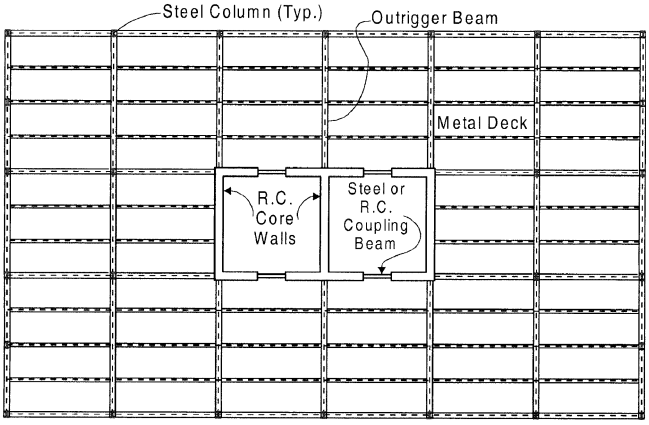

Fig. 1 Typical floor plan of a steel frame-reinforced concrete core wall hybrid system

loads. In such cases, the outrigger beams spanning between the central cores and perimeter frame are generally designed and detailed as beams with "shear connections". A typical shear connection is shown in Fig. 2. A steel plate with multiple headed shear studs is embedded in the core wall during casting, which may involve slip forming. After casting beyond the plate, the web of the steel beam is bolted to a "shear tab" which is already welded to the plate. Variations of this detail are common. The use of dual systems (i.e., a central core and steel perimeter frame) is more common in taller buildings, where the perimeter frames are engaged with the walls/cores as a means of reducing lateral deflections. For short-span outrigger beams, a single member that is connected to the cores through moment-resisting connections can achieve a sufficient level of stiffness. The span of most outrigger beams is, however, such that a single girder does not provide adequate stiffness, and other systems such as story-deep outrigger trusses are needed. The connection between the top and bottom chord of the truss is essentially similar to that used for shear connections between outrigger beams and core walls (Fig. 2). The connections between outrigger beams (including the floor slab) and core walls play a critical role in transferring the lateral forces to the cores.

A number of previous studies have examined multiple-anchor connections under combined shear

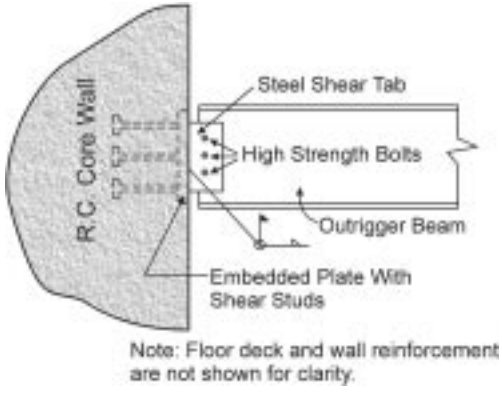

Fig. 2 Typical shear connections between outrigger beams and core walls

and moment (Cook and Klingner 1992, Hawkins *et al*. 1980, Roeder and Hawkins 1979, 1981). Fundamental differences exist between a typical multiple-anchor connection and that found in outrigger beam-core connections. Generally, strength of multiple anchors has been established through tests in which the concrete is not cracked, and transverse reinforcement is not provided around the studs. Experimental data regarding cyclic behavior of stud groups are also very limited. The loading in a typical outrigger beam-wall connection (i.e., a constant gravity shear and cyclic axial force due to floor diaphragm) has not been investigated in previous studies. In an effort to develop design and analytical models for outrigger beam-wall connections, the reported research was undertaken. The focus of this paper is on the first phase of the experimental component of the research.

2. Experimental program

The first phase of the reported research was focused on developing a basic understanding of behavior of stud groups under a constant shear force and a cyclic axial force. These specimens were intended to simulate shear connections between outrigger beams and core walls.

2.1. Test specimens

Seven 1/3-scale specimens were fabricated and tested. The test specimens were based on a 15-story prototype structure with a central core and steel perimeter frame, which was designed as part of the reported research. The general layout of the prototype structure was similar to that shown in Fig. 1, and is shown in the inset in Fig. 3. The distribution of axial forces in the designated collector element at each floor is plotted in Fig. 3. These forces were computed based on static analysis of the prototype structure under equivalent seismic lateral loads as defined in current building codes (NEHRP 1998). The core walls in the upper floors are not expected to experience major cracking and damage until the capacity of the studs in the connection is reached whereas the concrete in the connection region for the lower floors will likely undergo extensive damage. Larger forces in the collector elements in the lower floors and the possibility of damage in the wall around the connection will make the connections in

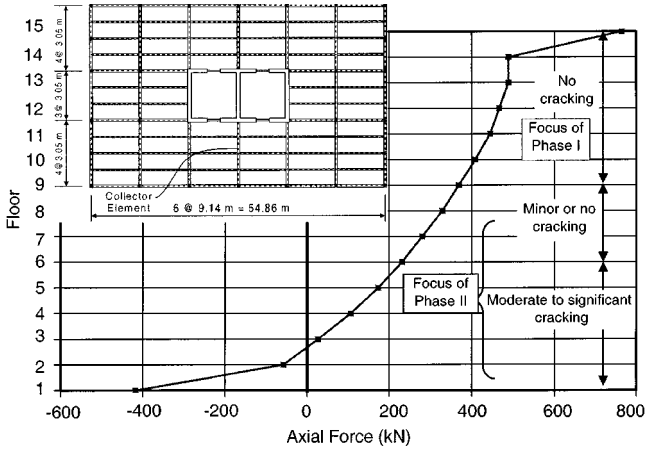

Fig. 3 Distribution of forces in collector element under equivalent seismic lateral loads

Table 1 Test matrix

Specimen	Stud Dimensions (mm)	f'_c (MPa)	Shear tab Yielding	No. of Studs	Stud plate Thickness (mm)	Shear plate Thickness (mm)	Boundary Element
1	12.7ϕ × 102	50.3	No	4	25.4	19.1	No
2	12.7ϕ × 102	50.3	No	6	25.4	19.1	No
3	12.7ϕ × 102	39.6	No	4	19.1	19.1	No
4	12.7ϕ × 102	39.6	No	4	19.1	19.1	Yes
5	12.7ϕ × 102	37.9	No	4	12.7	19.1	No
6	12.7ϕ × 102	37.9	No	4	12.7	19.1	No
7	12.7ϕ × 102	37.9	Yes	4	12.7	6.35	No

these floors more critical than those located in the upper floors. However, the walls in the lower floors will have boundary elements, which are anticipated to enhance the capacity of the studs as the transverse reinforcement in the boundary element confines the concrete around the studs. The walls in the upper floors will not likely have boundary elements; hence, the concrete surrounding the studs is not confined. Considering these issues, the behavior of the outrigger beam-wall connections in the upper floors is still critical and needs to be addressed. The focus of this paper is on the response of connections between core walls and collector elements in the upper floors.

In the first phase, the floor diaphragm was not included. The main test variables, summarized in Table 1, were (a) the number and size of studs, (b) the thickness of the embedded stud plate, (c) presence or lack of wall boundary element around the studs, (d) methodology for shear tab design. The general layout of the test specimens with and without boundary element is shown in Fig. 4. The thickness of the embedded stud plate for specimens 1 through 4 was arbitrarily selected as a large value so that the stud plate would be rigid as assumed in design model, which is described next. For the remaining specimens,

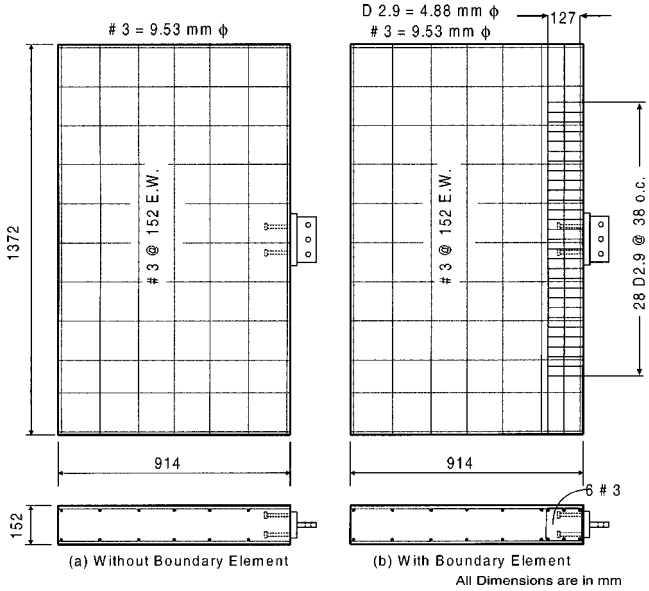

Fig. 4 General layout of test specimens

the plate thickness was calculated based on the prying action of the plate between the studs (LRFD 1994). Specimens 1 and 2 were intended to simulate the outrigger beam-core connections at different floors with different diaphragm forces. Specimen 3, which was essentially similar to specimen 1, was to provide benchmark data for comparison against specimen 4, which had boundary element, and to furnish additional experimental data. Specimens 5 and 6 were tested in order to evaluate the design procedure for calculating the stud plate thickness, and examine whether the distribution of forces among the studs corresponds to a rigid plate assumption. Based on the observations made from the first six specimens, the design approach was modified in order to dissipate the majority of the input energy through yielding of the shear tab. The validity of this new design method was examined through testing of specimen 7.

2.2. Design of specimens

Using standard similitude relationships, the equivalent 1/3-scale gravity shear and axial load resisted by the collector element in floor 7 were computed and used as design loads for the test specimens. This approach was followed in lieu of first designing the connections in the prototype structure and then scaling down the studs and other dimensions because of scaling issues of force mechanisms such as those in the stud groups used in the connection system. The specimens were designed based on the model shown in Fig. 5.

A previous study (Wang 1979) suggests that the design forces be increased by 50% to ensure a ductile failure. Hence, the gravity shear (V_u) and axial force representing the diaphragm force (T_u) were multiplied by 1.5. The stud plate was assumed rigid; hence, the forces will be distributed equally among various studs. The design is summarized as:

1) Knowing a preliminary layout of the studs, the shear capacity is calculated based on Precast Concrete Institute design equations (PCI 1999).

2) The numbers of studs in the compression region are calculated by assuming that only these studs resist the entire gravity shear.

3) Identical numbers of studs in the tension and compression regions are provided.

4) The depth of the compression block is computed from $k_d = (T_{acp}. - 1.5T_u)/ (0.85f'_c)b$ in which $T_{cap}.$ is

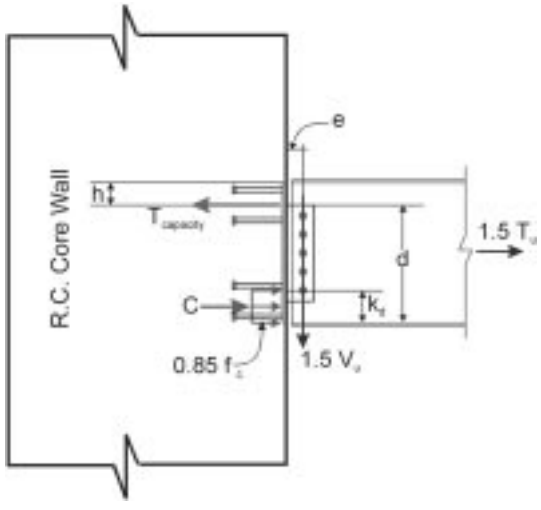

Fig. 5 Design model

the tensile capacity of the stud groups in tension.

5) The depth of the stud plate is taken as $d + h$ in which distance "d" is calculated from equilibrium of forces shown in Fig. 5 ($d = (1.5eV_u + 0.425bf'_c k_d^2 + 0.75hT_u)/(0.85bf'_c k_d + 0.75T_u)$), and the value of h is based on the stud diameter and edge distance of the stud. The edge distance should be large enough to allow welding of the studs. For the size of the studs used in this study, "h" was taken as about 13 mm.

6) The capacity of the studs under combined shear and tension is checked based on PCI interaction equations (PCI 1999).

2.3. Test setup

The specimens were tested as shown in Fig. 6. For simplicity, the specimens were tested in a horizontal position. Since the specimens in the first phase were intended to simulate outrigger beams in the upper floors of the prototype structure, the lateral deformation of the wall was not simulated to avoid damage in the wall around the connection in accordance with the expected behavior of the outrigger beams in the upper floors. A beam representing the outrigger beam was bolted to the shear tab, and was subjected to cyclic axial load (T) to replicate diaphragm forces. A constant gravity shear (V) was maintained throughout testing. The loading scheme is illustrated in Fig. 7. The gravity load shear was applied in a manner that the load line passed through the bolts between the outrigger beam and stud plate, see the inset in Fig. 6. Actual loads in outrigger beams are expected to produce some moments in the connection. In order to examine the cyclic behavior of stud groups under idealized conditions used in design models, the specimens were tested as shown to ensure that the connections would be subjected to shear and tension only.

The axial load regime consisted of a series of load-controlled cycles in which the magnitude was increased sequentially. The values of the compressive and tensile loads were identical until reaching 66.7 kN. Beyond this level, the magnitude of the compressive axial load was not increased due to concerns for buckling of the outrigger beam; however, the tensile axial load was increased until failure.

The specimens were instrumented to measure (a) the strain in each stud, (b) the movement of the stud

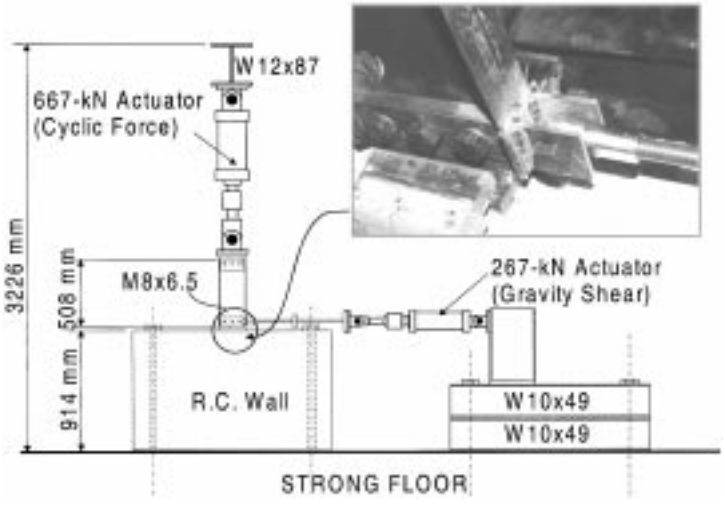

Fig. 6 Test setup

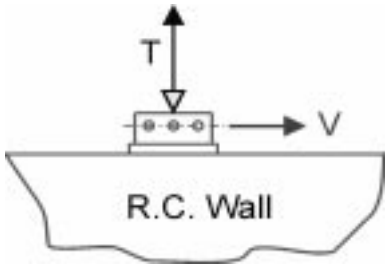

Fig. 7 Loading of test specimens

plate relative to the concrete wall, and (c) the applied load. The measured responses were supplemented with documentation of crack propagation and damage pattern.

3. Evaluation of test results

The failure of specimens 1, 2, 3, 5, and 6 was due to stud pull out as shown in Fig. 8. The boundary element in specimen 4 prevented a similar failure mode. As seen from Fig. 9, the failure of this specimen was due to fracture of weld between the studs and stud plate. In contrast to specimens 1, 2, 3, 5, and 6, the wall in this specimen did not exhibit any major damage until failure. At failure, the studs in specimen 4 had just yielded, whereas the maximum stud strains in specimens 1, 2, 3, 5, and 6 were about ¼ to ½ of the yield strain. These values are consistent with the observed modes of failure, i.e., the pull out failure is due to concrete failure at which the studs are not participating significantly. The test results clearly show the significance of transverse reinforcement in the boundary element around studs. The boundary element transverse steel confines the concrete around the studs, and prevents pull out of the studs. Such reinforcement will significantly enhance the capacity of studs, and should be taken into account in design equations.

Fig. 8 Typical failure mode involving stud pull out

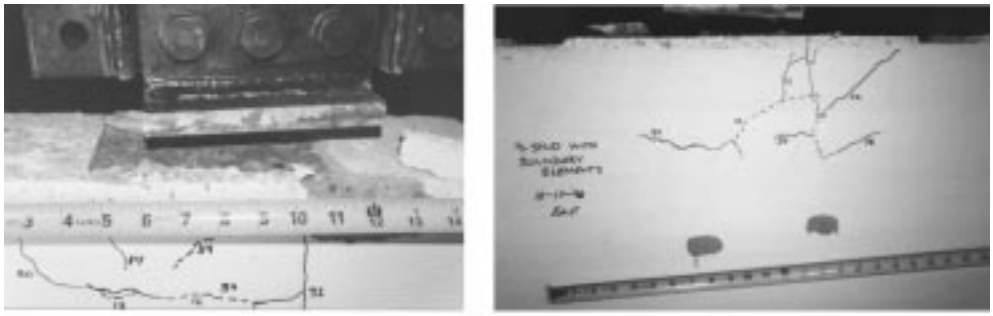

(a) Weld Failure (b) Damage Pattern at Failure

Fig. 9 Influence of boundary element in specimen No. 4 on mode of failure

A representative axial load-stud plate movement is shown in Fig. 10. Because of bending due to gravity shear, the south and north ends of the stud plate did not move equally. As evident in Fig. 8, the south end was not pulled up at failure, while the north end was pulled up due to the combined actions of the applied axial load and bending due to the gravity shear. On the other hand, the response of specimen No. 4, shown in Fig. 11, shows an appreciably large amount of upward movement of the embedded stud plate. The larger movement is attributed to slippage of the studs in the wall since the studs were essentially in the elastic range until failure. The boundary element had effectively prevented pullout of the studs despite relatively large slippage of the studs.

The design load for specimens 1, 3, 4, and 5 was 29.4 kN, and 44.5 kN for specimen 2. The maximum load resisted by specimens 1, 2, 3, 4, and 5 was 84.5 kN, 96.5 kN, 64.9 kN, 162 kN, and 88.1 kN, respectively. Clearly, the design method is adequate in terms of strength as the design method is apparently conservative in terms of the assumed distribution of forces among the studs, and the fact the design axial and shear forces are multiplied by 1.5. However, the observed modes of failure (stud pull out or weld rupture) are less than desirable, and need to be prevented through modification of the design methodology. A possible design method is to utilize the shear tab as the primary energy dissipation mechanism. That is, a capacity design method is followed to ensure that the capacity of the shear tab is developed before that of the studs. This method requires a good understanding of the

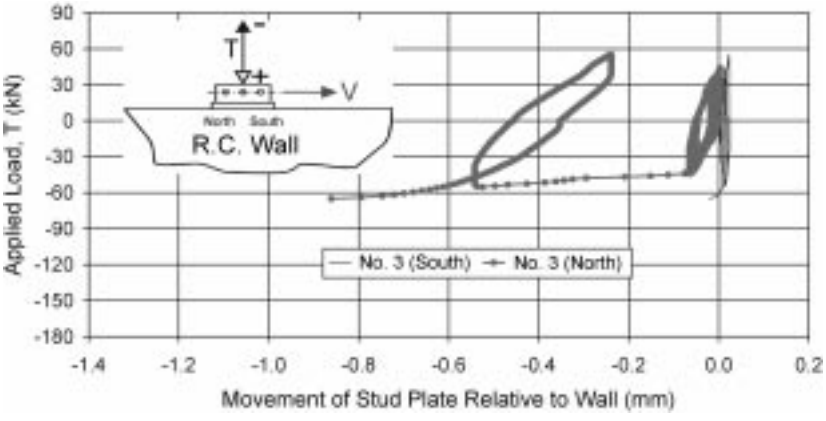

Fig. 10 Cyclic response of specimen No. 3 (without boundary element)

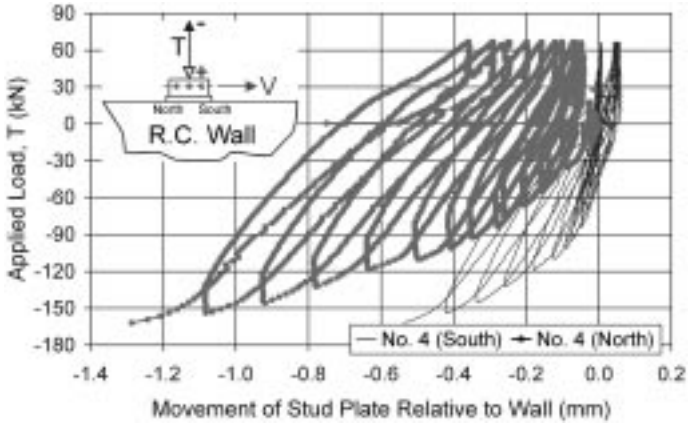

Fig. 11 Cyclic response of specimen No. 4 (with boundary element)

expected capacity of stud groups under combined actions of a gravity shear and cyclic axial force to ensure that studs do not fail before significant yielding and possible fracture of the shear tab.

4. Description of analytical model and evaluation of model

The analytical model shown in Fig. 12 is similar to the design model shown in Fig. 5. Based on PCI formulations (1999), tensile and shear capacities of the studs are computed. Using a liner distribution of concrete stress, the concrete stress is computed from $f_c = k_d V_u e / I_{transformed}$ in which k_d and $I_{transformed}$ are calculated based on standard techniques for a cracked transformed section in which the studs are considered as reinforcing bars, and the width of the stud plate is used as the beam width. For simplicity, the contribution of the studs in compression is ignored when k_d and $I_{transformed}$ are calculated. Knowing k_d, the value of C is $0.5bf_c\,k_d$, which is also equal to the tensile force (T). In the model, the contribution

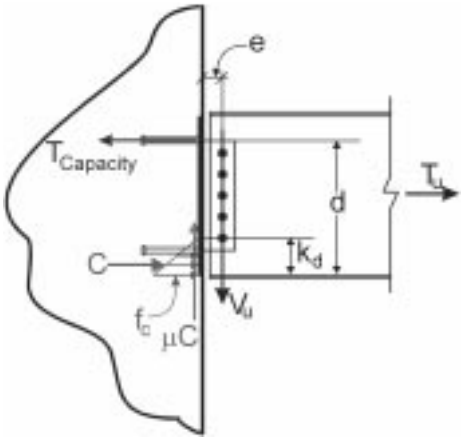

Fig. 12 Analytical model for computing capacity of studs

of friction between the embedded stud plate and concrete is also taken into account to reduce the shear demands. Since the experimental data show that the stud plates behave as rigid plates, the applied loads are divided equally among the studs. Studs in tension are most critical for pullout failure or stud fracture. The value of T_u, which can be resisted, is calculated from Eq. (1) or (2) depending on whether four studs or six studs are used, respectively. The factors of 0.5, 0.6, or 0.7 in the equations reflect the assumed distribution of the total axial and shear forces among the studs.

$$\left(\frac{T + 0.5T_u}{T_{capacity}}\right)^2 + \left(\frac{0.5(Vu - \mu C)}{nV_c}\right)^2 = 1 \tag{1}$$

$$\left(\frac{T + 0.3T_u}{T_{capacity}}\right)^2 + \left(\frac{0.3(Vu - \mu C)}{nV_c}\right)^2 = 1 \text{ or } \left(\frac{T + 0.7T_u}{T^*_{capacity}}\right)^2 + \left(\frac{0.7(Vu - \mu C)}{nV_c}\right)^2 = 1 \tag{2}$$

Note that in these equations, the value of gravity shear, V_u, is known. In Eq. (1), $T_{capacity}$ is the capacity of the studs in tension and V_c is the design shear capacity as computed from the applicable PCI equations, n is the number of studs, and μ is the coefficient of friction taken as 0.4 (Cook and Klingner 1992). The value of $T_{capacity}$ in Eq. (2) is also the capacity of the studs in tension, and $T^*_{capacity}$ is the capacity of the stud groups in tension. The smaller value of T_u from the two expressions in Eq. (2) is the controlling value.

The capacities of the specimens were calculated and compared against the measured values as summarized in Table 2. The aforementioned equations and proposed model are based on pullout failure of stud groups. Hence, the results for specimen 4 are not compared because the mode of failure in this specimen was different. With the exception of specimen 6, the model generally provides a very good estimate of the capacities. The calculated capacity of specimens 1, 2, 3, and 5 on the average is 98% of the measured value. In case of specimen 6, the measured capacity is 35% higher than the calculated value. The higher capacity is attributed to (a) unintended confinement of the stud head by the wall longitudinal bars (note that the studs in this specimen were longer than the previous studs), and (b) two of the wall web reinforcing bars were directly adjacent to the studs, and these bars could have increased the effective length of the studs (refer to Fig. 13).

5. Revised design methodology

As mentioned earlier, the revised design method is based on dissipating the energy through yielding of the shear tab. This goal is achieved by (a) computing the shear tab thickness required to resist the ultimate capacity of the stud groups as obtained from the analytical model, and (b) ensuring that the

Table 2 Comparison of measured and values computed based on proposed model

Specimen	Calculated (kN)	Measured (kN)	Calculated/Measured
1	87	84	1.028
2	100	97	1.031
3	72	65	1.100
5	87	88	0.991
6	137	173	0.788

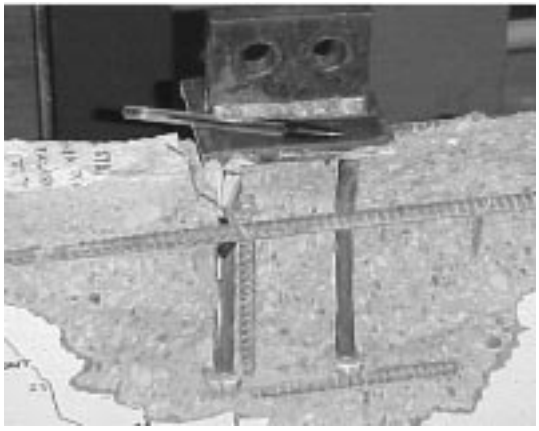

Fig. 13 Mode of failure for specimen 6

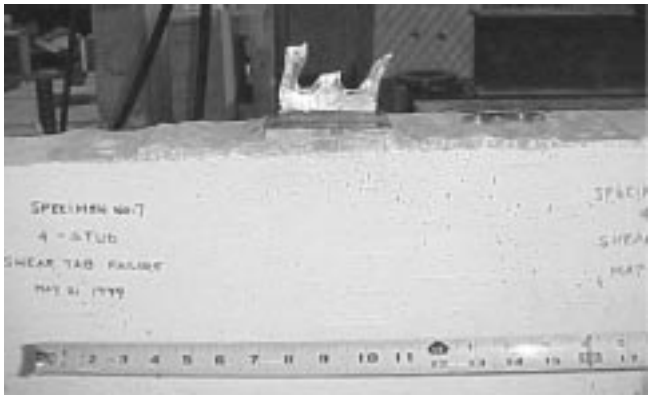

Fig. 14 Dissipation of energy in shear tab

plate thickness required to resist design loads is less than the thickness calculated in step (a). This design methodology was followed for specimen 7. The shear tab thickness in this specimen was 6.35 mm, which was about 1/3 of the thickness used for the first six specimens. The failure pattern shown in Fig. 14 clearly illustrates that the shear tab successfully resisted the applied loads, and the connection region did not experience any cracking or damage similar to what was observed for the other specimens. The mode of failure was ductile, and involved excessive yielding and eventual fracture of the shear tab. The failure load for this specimen was 163 kN, which was 5.5 times larger than the target design axial load of 29.4 kN (this load is 1/3-scale equivalent of the axial force in the selected collector element in the prototype structure). Considering the observed ductility and sufficient strength, the proposed design method for outrigger beam-core connections is apparently adequate.

6. Conclusions

Adequate cyclic performance of connections between outrigger beams and core walls is a prerequisite for satisfactory transfer of lateral loads to core walls, which are the primary lateral load resisting system in

a large class of structures. A coordinated experimental and analytical study at the University of Cincinnati is devoted to examining a number of issues critical to such systems. In this paper, the first phase of the research program is summarized. Seven specimens were fabricated and tested. Each specimen had a portion of the core wall, embedded plate with headed studs, a shear tab welded to the embedded plate, and an outrigger beam. The connections were subjected to simultaneous action of a constant gravity shear and a cyclic axial force simulating seismic forces in the floor diaphragm.

The specimens could develop and exceed the design loads; however, the failure due to pull out of the embedded failure was brittle. Boundary element transverse reinforcement around the studs approximately doubled the strength, and the failure was due to failure of the weld between the studs and embedded plate. Current equations for calculating the capacity of a single stud or stud groups need to be revised to include the additional capacity due to the confinement provided by confinement from wall boundary element transverse reinforcement.

In order to prevent brittle failure modes, a revised design method is proposed in which the input energy is dissipated through yielding of the shear tab. As part of this method, a model for calculating the expected capacity of stud groups was developed. This model could very closely replicate the measured capacities. A specimen designed based on the revised design method performed satisfactorily. The input energy was effectively dissipated through yielding of the shear tab, and the connection region did not experience any damage. Using the developed design method, outrigger beam-wall connections can be designed with sufficient ductility.

Acknowledgements

The reported research was funded by the National Science Foundation (Grant CMS-9632496) as part of the fifth phase of US-Japan cooperative research program on composite and hybrid structures. Dr. C. Liu is the program director.

References

Cook R.A., Klingner, R.E. (1992). “Ductile multiple-anchor steel-to-concrete connections”, *J. Struct. Div.*, ASCE, **118**(6), 1645-1665.

Hawkins, N.M., Mitchell, D., and Roeder, C.W. (1980). “Moment resisting connections for mixed construction”, *Eng. J.*, AISC, **17**(1), 1-10.

LRFD (1994). “Load and resistance factor design - Volume I”, American Institute of Steel Construction, Chicago, Illinois.

NEHRP, 1998, *Recommended Provisions for Seismic Regulations for New Buildings and Other Structures* (FEMA 302) and *Commentary* (FEMA 303), Building Seismic Safety Council, Washington, D.C.

PCI Design Handbook - Precast and Prestressed Concrete (1999). Precast Concrete Institute, Chicago, IL.

Roeder, C.W. and Hawkins, N.M. (1979). “Connections between steel beams and concrete walls”, *ASCE Convention and Exposition*, Atlanta, 23-25.

Roeder, C.W. and Hawkins, N.M. (1981). “Connections between steel frames and concrete walls”, *Eng. J.*, AISC, **18**(1), 22-29.

Wang, M. (1979). “The behavior of steel structure to shear wall connections under tension”, Masters Thesis, University of Washington, Seattle, Washington.

CU